Electronic Supplementary Material (ESI) for ChemComm.

Supporting Information

The novel application in zinc-air battery of imidazole-based ligand templated borates

Yan-Ling Deng,‡a An-Na Chen,‡a Shu-Sheng Xin,a and Chun-Yang Pan*a

[a] *School of Chemical Engineering and Light Industry, Guangdong University of Technology, Guangzhou, Guangdong 510006, China*; Tel: +86-020-39322231 Fax: +86-020-39322231.
*Corresponding author: Chun-Yang Pan, E-mail: panchuny@gdut.edu.cn
‡These authors contributed equally.

Experimental Section

Synthesis of 1 and 2

1 was obtained by solvothermal method. H_3BO_3 (0.972 mmol) and $Co(SO_4)_2$ (0.870 mmol), were dissolved in pyridine (2 mL). After the solution was stirred for 2 h, 1-Ethylimidazole was added. The resulting homogeneous emulsion was encapsulated into a 25 ml stainless steel reactor and heated at 180 °C for 7 days. Then the reactor was gradually cooled to room temperature, and purple crystals of **1** were obtained (yield 51 % based on H_3BO_3). Elemental Analysis for **1**. Calcd: C 25.6, H 4.1, N 11.9 wt%; Found: C 24.5, H 4.7, N 11.2 wt%.

2 was made by the solution evaporation method. 1-Methylimidazole (1 mL), $Ba(OH)_2$ (5.76 mmol) and $Ga_2(SO_4)_3$ (2.19 mmol) were added to H_2O 20 mL and stirred for 40 min. The filtrate was retained by filtration, and boric acid (13.9 mmol) was added to the filtrate. After stirring for 30 minutes, the solution was placed in a beaker for 20 days to obtain colorless transparent crystals. Transparent colorless crystals **2** were recovered by filtration, washed with ethanol, and air-dried (42% yield, calculated as H_3BO_3). Elemental Analysis for **2**. Calcd: C 19.3, H 4.9, N 11.2 wt%; Found: C 18.6, H 5.3, N 10.8 wt%.

Materials and characterization

$Co(SO_4)_2·7H_2O$ (Aladdin, 98%), $Ga_2(SO_4)_3$ (Macklin, 97%), $Ba(OH)_2$ (DAMAO, AR), 1-methylimidazole (Aladdin, 98%), 1-ethylimidazole (Aladdin, 98%), pyridine (Macklin, 99.5%), and H_3BO_3 (Aladdin, 99.5%). All chemicals are commercially available and do not require further purification.

Infrared spectra in the 400-4000 cm^{-1} range were obtained by pressing samples on KBr pellets on a Themor-Filsher iS50R spectrometer. Using Cu Kα radiation, powder X-ray diffraction (PXRD) data at an angle of $2\vartheta = 5\text{-}50°$ was recorded on the PW 3040/60, PANalytical, Almelo, Netherlands powder diffractometer. The solid-state UV-vis-NIR absorption spectra was performed on the Shimadzu UV-3600 plus spectrophotometer that contained an integrating sphere at room temperature, which used $BaSO_4$ as powder samples with the standard of 100% reflectance. Elemental analyses (C, H and N) were carried out on a PerkinElmer 2400 elemental analyzer. The

EDX mapping of the sample was obtained by using a xenon lamp as the light source and a transmission electron microscope device on a Hitachi SU8100 instrument. The specific surface area and pore size distribution of the samples were measured on the Micrometer ASAP 2460 instrument. The nitrogen adsorption-desorption isotherm curve was obtained by BET-BJH method.

Heat treatment. 40 mg of **1** and 10 mg of carbon black were mixed and grinded well, then the mixture was heated at 150 °C in N_2 atmosphere, at the heating rate of 5 °C min^{-1} for 2 h. After cooling to room temperature, the mixture was named as 1-CoB5/150. 1-CoB5/300, 1-CoB5/450, 1-CoB5/600, 1-CoB5/750 and 1-CoB5/900 were obtained as for 1-CoB5/150 except that the temperature was changed to 300, 450, 600, 750 and 900 °C, respectively. **2** was heated through a process similar to that for **1**. 2-based electrocatalysts were obtained, which were named 2-GaB6/150, 2- GaB6/300, 2- GaB6/450, 2-GaB6/600 and 2- GaB6/750, respectively.

Electrochemical Measurements. All electrochemical measurements of ORR are performed at room temperature in a conventional three-electrode system on a computer-controlled electrochemical workstation. To examine the ORR activity, linear sweep voltammetry (LSV) measurements on the rotating disk electrode (RDE) were performed in an O_2-saturated 1 M KOH solution at a rotation speed of 1600 rpm with a scan rate of 5 mV/s. In the typical method for catalyst ink preparation, 5 mg of synthesized catalyst powder was dispersed in solution of 1 ml of ethanol and 20 µl of nafion solution (5 wt %) for an hour. Then, 5 µl of catalyst ink was dropped on the surface of the working electrode, and after drying, repeat the above operation for three times. Finally, a working electrode was prepared on the RDE for testing.

During the test of zinc-air battery, the oxide layer on the surface of zinc plate was removed by sandpaper with a thickness of 0.5 mm, which was used as anode. The catalyst was loaded on carbon paper and used as air cathode. The electrolyte was 6 M KOH and 0.2 M $Zn(CH_3COO)_2$ solution. The air electrode was prepared by dispersing 6 mg heat-treated cobalt borate and gallium borate catalysts in 2000 µL ethanol and 12 µL 6 % PTFE solution, respectively, and ultrasonic treatment for 30 min to obtain catalyst dispersion. Then the prepared catalyst dispersion was sprayed on the carbon paper, and the open circuit voltage, cycle stability and constant current charge and discharge performance were tested on the battery test system BTS-5V10 mA after natural drying.

Determination of crystal structure

Diffraction data were measured on a Rigaku Mercury CCD diffractometer, using graphite monochromatic Mo $K\alpha$ (K=0.71073 Å) radiation, and all absorption corrections were performed using the Multiscan program.[1-2] The structure is solved by the direct method, and the full matrix least squares fitting of F^2 is refined by the *Olex2* and *OlexSys* programs.[3] All H atoms were geometrically fixed at calculated distances and allowed to ride on the non-H parent atoms. All non-H atoms were anisotropically refined. SQUEEZE program was used to remove the contributions of disordered solvent (For **2**, during the SQUEEZE process, a solvent mask was calculated and 134 electrons were found in a volume of 507 $Å^3$ in 1 void per unit cell. This is consistent with the presence of 6.7[H_2O] per asymmetric unit which account for 134 electrons per unit cell.).[4] Crystallographic data and the structure determination for **1** and **2** are summarized in **Table S1**. The crystallographic data for the structure of **1** and **2** in this paper have been deposited in the Cambridge Crystallographic Data Centre, CCDC, 12 Union Road, Cambridge CB21EZ, UK. A copy of the data can be obtained free of charge by quoting the depositary number CCDC-2284602 (**1**) and CCDC-2284917 (**2**).

Table S1 Crystal data and structure refinement for **1** and **2**

Compound	**1**	**2**
Empirical formula	$C_{20}H_{38}B_{10}Co_2N_8O_{20}$	$C_{24}H_{52}B_{14}Ga_2N_{12}O_{32}$
Temperature/K	150.0	150
Formula weight	936.54	1311.55
Crystal system	Triclinic	Triclinic
Space group	*P*-1	*P*-1
a/Å	11.5059(5)	12.0536(8)
b/Å	11.8461(4)	12.2219(7)
c/Å	15.9399(7)	12.5599(7)
α/°	89.3770(10)	93.947(2)
β/°	87.352(2)	112.798(2)
γ/°	67.3260(10)	92.145(2)
V/Å^3	2002.50(14)	1697.56(18)
Z	2	1
ρ_{calc}(g/cm^3)	1.553	1.283
2ϑ range for data	4.504 to 51.394	6.012 to 50.156
Reflection collected	47519	45657
F(000)	956	668
Independent reflections	7551	5929
limiting indices	$-14 \le h \le 14$, $-14 \le k \le 14$, $-19 \le l \le 19$	$-14 \le h \le 14$, $-14 \le k \le 14$, $-14 \le l \le 14$
GOF on F^2	1.125	1.027
final R indices [$I > 2\sigma(I)$]	$R_1 = 0.0553$, $wR_2 = 0.1336$	$R_1 = 0.0343$, $wR_2 = 0.0801$

Table S2 H-Bs for **1**

D–H···A	d(D–H) (A˚)	d(H···A) (Å)	d(D···A) (Å)	∠D—H···A (°)
O3–H3···O16[1]	0.84	1.88	2.711(2)	166
O7–H7···O6[2]	0.84	1.89	2.718(2)	167
O13–H13···O14[3]	0.84	1.94	2.773(2)	172
O20–H20···O4[4]	0.84	1.92	2.758(2)	170

[1]X+1, Y-1, Z; [2]-X+2, -Y, -Z+1; [3]-X+1, -Y+2, -Z; [4]X-1, Y+1, Z

Table S3 H-Bs for **2**

D–H···A	d(D–H) (Å)	d(H···A) (Å)	d(D···A) (Å)	∠D—H···A (°)
O2–H2B···O5	0.82	1.87	2.682(3)	171
O3–H3A···O8	0.82	1.95	2.753(3)	167
O7–H7···O12[2]	0.82	1.85	2.643(2)	163
O15–H15···O9[1]	0.82	1.90	2.709(2)	168
N2–H2···O14[1]	0.86	1.87	2.701(3)	161

[1]-X,1-Y,1-Z; [2]1-X,1-Y,1-Z

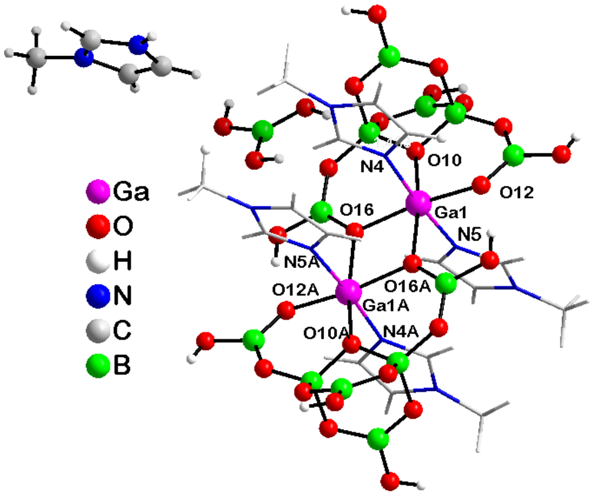

Fig. S1 The asymmetric structural unit of **2**, the atoms with lable "A" generated by symmetric operation.

Each Ga atom is surrounded by four oxygen atoms from $[B_6O_9(OH)_4]^{4-}$ group and two nitrogen atoms from 1-MI molecule to form a six-coordinated mode, and then form a $C_{16}H_{32}B_{12}Ga_2N_8O_{26}$ complex by symmetric operation, which lies about an inversion centre.

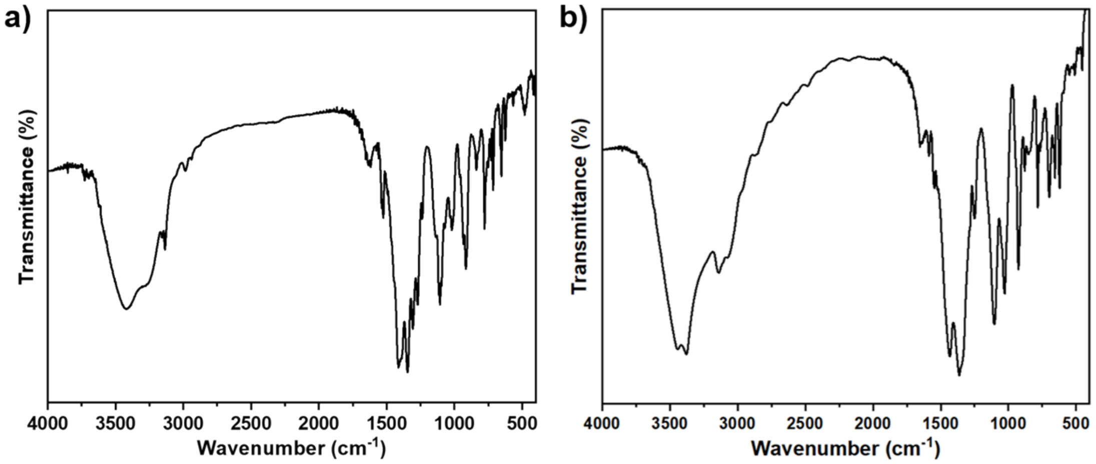

Fig. S2 The FTIR spectra of **1**(a) and **2**(b).

The FTIR spectrum of **1** and **2** are shown in **Fig. S2**. The wider absorption peaks at 3413 cm^{-1}(**1**) and 3434 cm^{-1}(**2**) correspond to the asymmetric stretching vibration of O-H. The symmetrical stretching of the C-H and N-H groups may be observed in the range of 3150-2850 cm^{-1}. The above resonance signals further confirmed the existence of organic components and O-H. The absorption peak at about 1346 cm^{-1}(**1**) and 1351 cm^{-1}(**2**) correspond to the B-O asymmetric stretching vibration of the BO_3 groups. The B-O asymmetric stretching vibration of the BO_4 groups appear in the vicinity of 1106 cm^{-1}(**1**) and 1093 cm^{-1}(**2**).

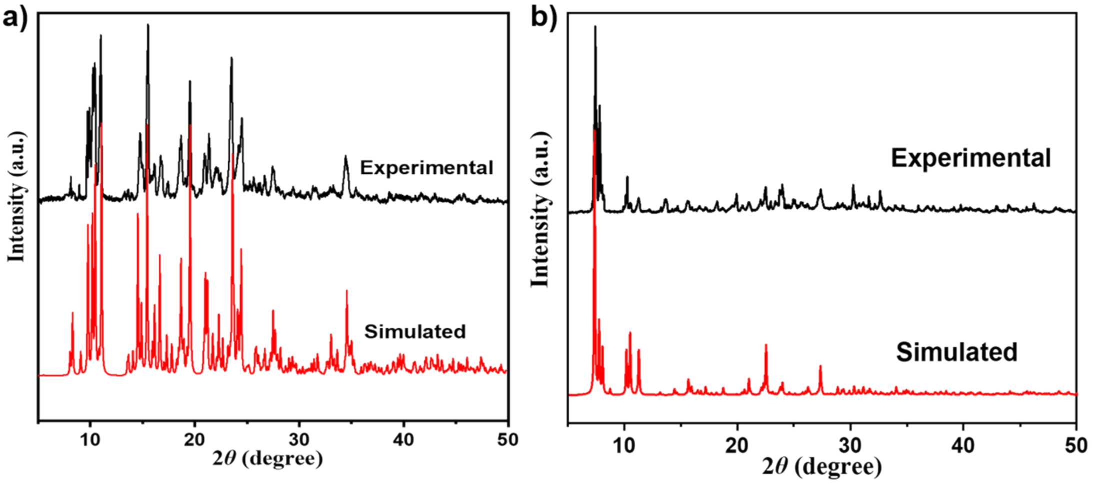

Fig. S3 The PXRD patterns of **1**(a) and **2**(b).

The PXRD pattern of the simulated pattern based on the single crystal structure of **1** and **2** are shown in **Fig. S3**. The PXRD spectrum obtained by the experiment is in good agreement with the simulated spectrum obtained from the single crystal structure, indicating that the phase-purity of **1** and **2**. There is a slight difference in the reflection intensity between the simulated pattern and the experimental pattern, which is due to the change in the preferred orientation of the powder sample.

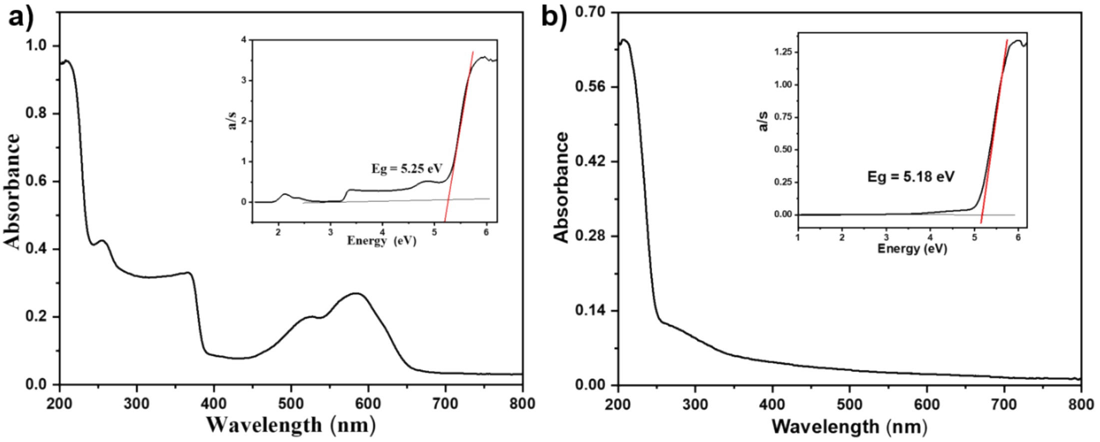

Fig. S4 The solid-state UV-vis-NIR absorption spectra of compound **1**(a) and **2**(b) (the insets show the Tauc plots of α/S vs. photon energy).

The solid-state UV-vis-NIR absorption was performed to study the optical properties of **1** and **2**. According to the Kubelka–Munk formula: $\alpha/S = (1 - R)^2/2R$ (α is the absorption coefficient, S is the scattering coefficient, and R is the reflectance).[5] As shown in **Fig. S4**, the band gap of **1** and **2** are about 5.25 and 5.18 eV, which show that these materials can be used as the wide bandwidth semiconductor materials.

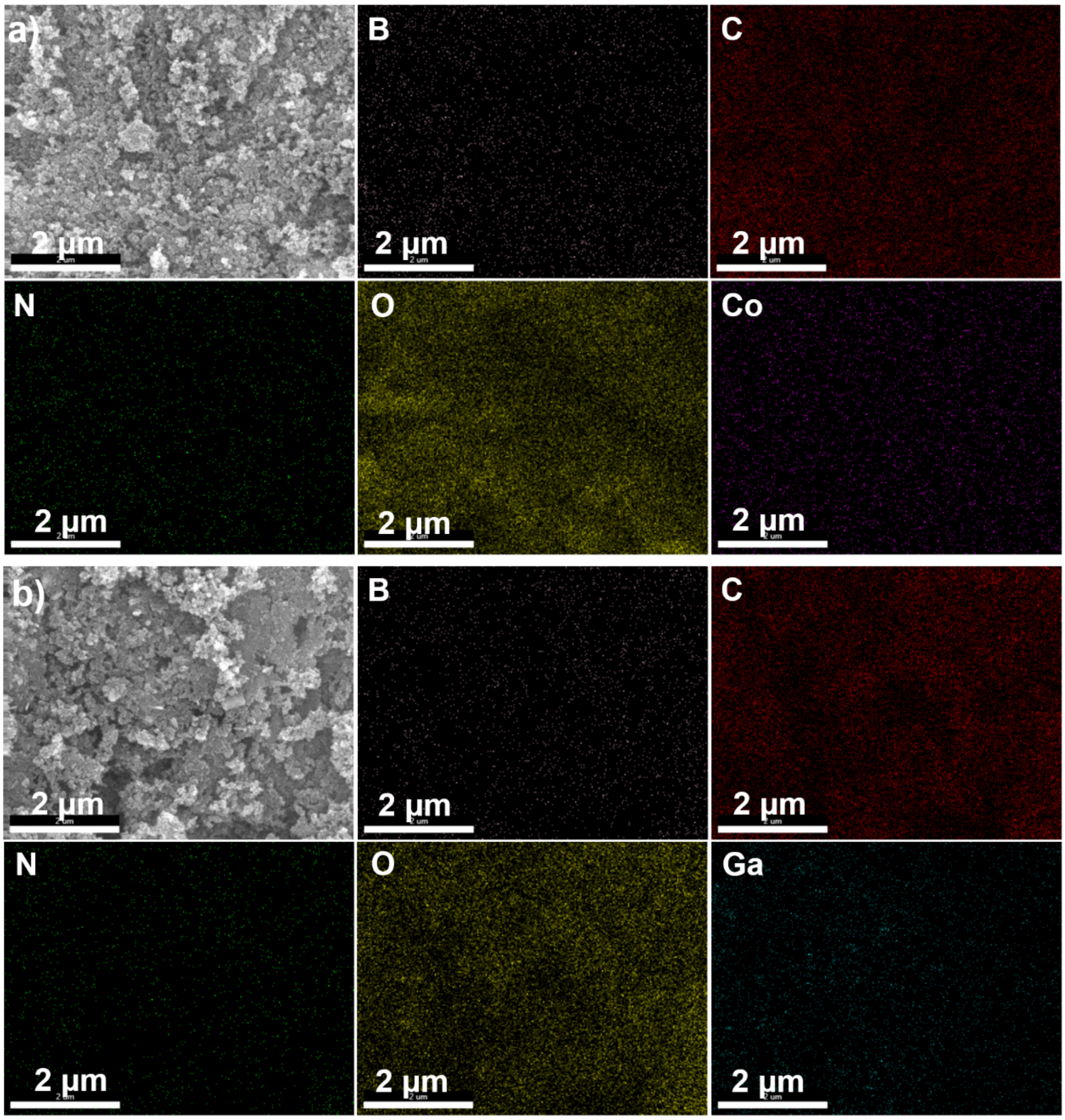

Fig. S5 a) The EDX mapping of 1-CoB5/750; b) The EDX mapping of 2-GaB6/600

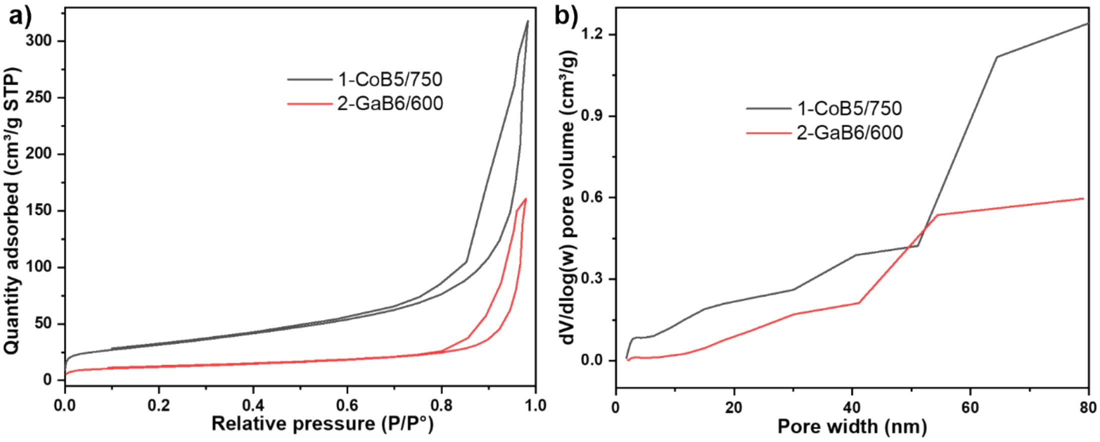

Fig. S6 a) N_2 adsorption-desorption isotherm curves of 1-CoB5/750 and 2-GaB6/600 electrocatalyst; b) BJH pore-size distribution profiles of 1-CoB5/750 and 2-GaB6/600 electrocatalyst.

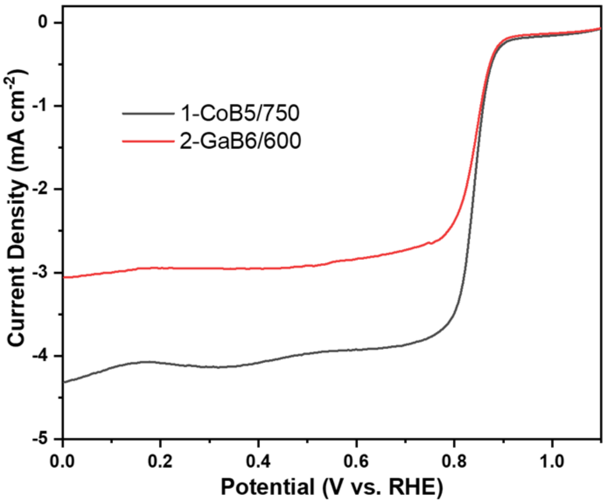

Fig. S7 a) The LSV curves of 1-CoB5/750 and 2-GaB6/600 (5 mV s^{-1}, 1600 rpm)

Notes and references

1. G. M. Sheldrick, *Acta Crystallogr., Sect. A: Found. Adv.*, 2015, **71**, 3-8.
2. G. M. Sheldrick, *Acta Crystallogr., Sect. C: Struct. Chem.*, 2015, **27**, 3-8.
3. O. V. Dolomanov, L. J. Bourhis, R. J. Gildea, J. A. K. Howard, H. Puschmann, *J. Appl. Crystallogr.*, 2009, **42**, 339-341.
4. A. L. Spek, *Acta Crystallogr. Sect. C: Struct. Chem.*, 2015, **71**, 9-18.
5. W. M. Wendlandt and H. G. Hecht, *Reflectance Spectroscopy*, Interscience Publishers, New York, 1966.